CrossMark

ORIGINAL PAPER

Thymine chitosan nanomagnets for specific preconcentration of mercury(II) prior to analysis using SELDI-MS

Hani Nasser Abdelhamid[1,2] · Yu Chih Lin[1] · Hui-Fen Wu[1,3,4,5]

Abstract Laser desorption-ionization mass spectrometry (LDI-MS) is used to determine Hg(II) ions by using thymine-modified chitosan-coated magnetic nanoparticles (TCTS). TCTS nanoparticles are characterized using transmission electron microscopy, X-ray diffraction, UV-vis absorption, infrared spectroscopy and LDI-MS. TCTS acts as a preconcentration probe, supports surface enhanced LDI-MS (SELDI-MS) and acts as a capping agent for Hg(II). The separation of Hg(II) via this method combined with SELDI-MS provides a sensitive and selective tool for inexpensive and fast (5 min) detection of Hg(II) with limit of detection down to 0.05 nmol for environmental samples such as tap and sea water.

Hani Nasser Abdelhamid and Yu Chih Lin are co-first author with equal contribution

✉ Hui-Fen Wu
hwu@faculty.nsysu.edu.tw

[1] Department of Chemistry and Center for Nanoscience and Nanotechnology, National Sun Yat-Sen University, Kaohsiung 804, Taiwan

[2] School of Pharmacy, College of Pharmacy, Kaohsiung Medical University, Kaohsiung 800, Taiwan

[3] Institute of Medical Science and Technology, National Sun Yat-Sen University, Kaohsiung 804, Taiwan

[4] National Sun Yat-Sen University and Academia Sinica, Kaohsiung 80424, Taiwan

[5] Department of Chemistry, Assuit University, Assiut 71515, Egypt

Introduction

Mercury (Hg) is one of the most toxic and dangerous heavy metal elements in the environment [1, 2]. Mercury species cause serious diseases/syndromes such as neurological damage resulting in symptoms such as mental retardation, seizures, vision and hearing loss, delayed development, language disorders and memory loss [1, 2]. The World Health Organization (WHO) states the maximum allowable level of inorganic mercury as no more than 6 ppb (30 nM) in drinking water. In USA, approximately 50 tons of mercury is released into the atmosphere annually from coal-fired power plants (represents one third of the U.S. anthropologic mercury emissions) [3]. Release of mercury to the environment is a serious problem due to the persistence in the environment and the circulation between air, water, sediments, soil and living creatures. Mercury species travel long distances to areas far from the area of production or use. Lamborg et al. reported approximately 150% an increase in the amount of mercury in thermocline waters and have tripled the mercury content of surface waters compared to pre-anthropogenic conditions [4]. The release of mercury emission should be reduced and monitored carefully [5]. Thus, analytical tools that provide sensitive, selective and fast monitor for mercury ions (Hg(II)) are highly required.

Toward this high demand, there are many methods for the detection of mercury(II) ions including, for example, atomic absorption spectroscopy (AAS) [6], inductively coupled plasma mass spectrometry (ICP-MS) [7], atomic fluorescence spectrometry (AFS) [8] and others [9–11]. However, these techniques require complicated procedure for the sample

preparation, are expensive, require bulky instruments and professionally trained person. Alternative techniques include fluorescence [12–14], plasmonic gold nanoparticles, aptamer based colorimetry [15, 16], surface enhanced Raman spectroscopy (SERS) [17, 18] and mass spectrometry (MS) were reported [19]. Nanoparticle based technologies improved and enhanced the limit of detection [20–22]. The detection limit of time of flight mass spectrometry (TOF-MS) with ionization process is often ppb or less. The limit of detection can be improved using simple preconcentration nanoprobe such as magnetic nanoparticles. Magnetic nanoparticles based nanocomposite (xanthate functionalized magnetic graphene oxide (Fe_3O_4-xGO) were reported for mercury separation [23]. These new technologies provided selective separation or sensing for mercury species. Applications of functionalized magnetic nanoparticles [24] and magnetic chitosan composites (MCCs) [25] for the removal of toxic metal and dyes from aqueous solutions were reviewed.

Herein, we report on a simple, specific, sensitive and fast method for separation and specific detection of mercury(II) ions from aqueous media. Thymine modified chitosan magnetic (Fe_3O_4) nanoparticles (TCTS nanomagnets) were synthesized and characterized using TEM, XRD, FTIR, and UV-vis absorption. TCTS nanomagnets offered a selective, sensitive and fast platform for the detection of Hg(II) ions using surface enhance laser desorption/ionization mass spectrometry (SELDI-MS). TCTS offered a selective nanoprobe for preconcentration; served as platform for surface enhanced LDI-MS (SELDI-MS) and capping agents for Hg(II) ions. TCTS provided selective and sensitive platform for Hg(II) ions in tap and sea water. Furthermore, magnetic nanoparticles could work as a soft ionization method for low mass range (50–500 m/z) where conventional organic matrix causes interferences at the interested mass range.

Materials and methods

Chitosan (molecular weight > 75,000 g·mol^{-1}), sulfuric acid, nitric acid were purchased from Baker (India, http://jtbaker.com/). $KMnO_4$, $FeCl_2·4H_2O$, $Cu(NO_3)_2$, $Mg(NO_3)_2$, $Ni(NO_3)_2$, $HgCl_2$, NaCl, KCl, $AlCl_3$, and $SnCl_4$ and $FeCl_3·6H_2O$, were purchased from Riedel-de Haën (Seelze, Germany, http://www.riedeldehaen.com/). 2,5-DHB (2,5-dihydroxybenzoic acid) and natural graphite (−20 + 84 mesh, 99.9%) were purchase from Alfa Aeser (Great Britain, https://www.alfa.com/en/). Methanol (HPLC grade) and potassium permanganate were purchased from Merck. Co (USA, http://www.merck.com/index.html). Deionized water obtained from a Milli-Q Plus water purification system (Millipore, Bedford, MA, USA, https://www.merckmillipore.com) was used for all experiments.

Synthesis of chitosan modified magnetic nanoparticles (TCTS)

Chitosan modified magnetic nanoparticles (TCTS) were synthesized with the modification of our previous report [26]. $FeCl_2·4H_2O$ (0.63 g), and $FeCl_3·6H_2O$ (1.73 g) were added to chitosan solution (0.2 g, 25 mL H_2O, 1 mL acetic acid). The mixture was stirred for 12 h at room temperature. Then, the solution was purged with nitrogen gas and stirred in water bath at 90 °C for 3 h (pH was adjusted to 9 using NH_4OH). The precipitate was separated by external magnets and was dried in a vacuum oven. The material was re-dispersed in solution of thymine (2 g, 25 mL H_2O) and was stirred for 12 h. The material was collected using external magnetic field and washed with water (2 × 30 mL).

Synthesis of graphene oxide and graphene

Graphene oxide was synthesized using the Hummers method [27, 28]. The material was reduced using hydrazine solution and applied for graphene assisted laser desorption/ionization mass spectrometry (GALDI-MS) as described in our previous report [19]. The material was characterized using TEM, SEM, EDX, Raman spectroscopy, fluorescence, and UV-vis absorption, as mentioned in our previous papers [29, 30].

Instruments

UV-vis absorption measurements were undertaken in an UV spectrophotometer (Perkin Elmer 100, German). Fourier transform infrared (FT-IR) spectra of chitosan and TCTS were recorded on a FT-IR spectrometer (Spectrum 100, Perkin Elmer, USA). The size and morphology of magnetic nanoparticles were determined using transmission electron microscope (TEM, JEOL-301, Tokyo, Japan). Matrix assisted laser desorption/ionization time of flight mass spectrometry (MALDI-TOF-MS) analysis were performed by employing positive mode on a time-of-flight mass spectrometer (Microflex, Daltonics Bruker, Bremen, Germany). Instrumental parameters were described in our previous reports [31–36]. The spectra were calibrated using DHB peaks (M. Wt 154 g·mol^{-1}, [DHB + Na]$^+$ at 177 Da and [DHB-H_2O + H]$^+$ at 137 Da). All experiments were repeated at least three times to confirm the reproducibility.

Selectivity measurement

Metal ions such as Fe(III), Fe(II), Cu(II), Mg(II), Ni(II), Hg(II), Na(I), K(I), Al(III), and Sn(IV), were mixed in one solution (1 mg for each metal, V_{total} 10 mL). Simply, 10 μL of this solution was mixed with thymine (20 μL). Then, 10 μL of this mixture was mixed with nanoparticles (10 μL) prior to spotting on MALDI plate. Another 10 μL of the metal

solution was mixed with thymine (20 μL), nanoparticles (10 μL) and DHB matrix (10 μL, 50 mM, methanol:water 50:50 (vol:vol)). Then, 10 μL was spotted on MALDI plate. The same experiment was performed without nanoparticles and in the presence of DHB. The experiment was repeated for monovalent, divalent and trivalent metal species.

Sensitivity measurement

To investigate the sensitivity of the present protocol, Hg(II) ions with concentration (1, 10, 50, 100, 500, 1000, 2000, 3000 μM) were investigated. 10 μL of TCTS nanomagnet was added to the previous solutions individually and separated using external magnetic field. The separated species re-dispersed in 10 μL of highly distilled water and was spotted on MALDI-MS standard stainless plate.

Analysis of real sample

Two different samples (tap and sea water) were used as real samples. Different volumes (1, 10, 50, 100, 500, 1000, 2000, 3000 μL) of Hg(II) (10 mM) were spiked in tap and sea water (3 mL). Then, 10 μL of TCTS solution was added and separated using external magnetic field. The separated material was re-dispersed and spotted in MALDI-MS plate as described above. The experiments were repeated with and without DHB matrix (50 mM, methanol:water ratio was 1:1 (vol:vol)).

Results and discussion

Material characterizations

Thymine modified chitosan magnetic nanoparticles (TCTS) was synthesized using hydrothermal method as shown in Fig. 1a. The function groups of chitosan serve as chelating agents for the ions of Fe(II) and Fe(III) that were used to prepare magnetic nanoparticles (Fe_3O_4). These function groups are also able to coordinate to thymine molecules. The material was characterized using TEM (Fig. 1(b-c)), XRD (Fig. 2a), FTIR (Fig. 2b), UV-vis absorption (Fig. 2c), and laser desorption/ionization mass spectrometry (LDI-MS, Fig. 2d). TEM images for chitosan modified magnetic nanoparticles (CTS@Fe_3O_4, Fig. 1b) and thymine chitosan nanomagnets (TCTS nanomagnets, Fig. 1c) reveal the size and morphology of the prepared materials. Data shows that the size of magnetic nanoparticles within chitosan modified magnetic nanoparticles (CTS@Fe_3O_4, Fig. 1b) is about 10 nm. The magnetic nanoparticles undergo aggregation after the modification with thymine molecules due to the interactions within the material (Fig. 1c). XRD (Fig. 2a) confirms the formation of magnetic nanoparticles modified with chitosan.

Figure 2a shows good agreement of the experimental pattern with the simulated diffraction pattern. The five characteristic peaks of Fe_3O_4 at Bragg angles (2θ) of 30.12°, 35.57°, 37.08°, 43.13°, and 47.27° were indexed using Joint Committee on Power Diffraction Standards database (File No. 250540) to the indices (220), (311), (222), (400), and (331), respectively. The absence of chitosan diffraction peak at Bragg angle (20.1°) may be due to the low concentration or the absence of crystallinity.

FTIR spectra reveal the differences in the chemical function groups of chitosan, as well as for the materials after capping of magnetic nanoparticles. FTIR (Fig. 2b) shows the characteristic peaks of chitosan before and after modification with magnetic nanoparticles. Chitosan has a broad peak at 3440 cm^{-1} corresponding to N—H stretch (overlapped with O—H stretch), 2800 cm^{-1} (C—H stretching vibration), 1659 cm^{-1} (amide band I), 1591 cm^{-1} (amide II band, N–H stretch), 1217 cm^{-1} (can be attributed to C—N stretching vibration, amino group band), 1096 cm^{-1} (the stretching vibration mode of the hydroxyl group) and 1378 cm^{-1} (C—H symmetrical angular deformation). The increase of the sharpness of amide peak at 1659 cm^{-1} due to the modification and interactions of chitosan function groups with thymine. Chitosan function groups show changes after capping with the core of magnetic nanoparticles. In addition to the characteristic absorption bands of the functional groups of chitosan, a new peak at 660 cm^{-1} is observed and that refers to Fe—O band. This observation proves the successful formation of magnetic nanoparticles embedded inside chitosan nanoparticles.. The surface of iron oxide is charged by negative charges that interacts with the positive charge of TCTS (—NH_3^+ groups, electrostatic forces) [37, 38]. The presence of O—H groups in chitosan backbone and N—H groups in thymine reinforce the interactions through hydrogen bonds.

UV-vis absorption of thymine modified chitosan nanomagnets (TCTS@Fe_3O_4) was investigated as shown in Fig. 2c. UV-vis absorption (Fig. 2c) shows broad absorption at 200–700 nm with maximum absorption at 200 nm and 250 nm. The material offers absorption at wavelength of 337 nm that matches with the laser wavelength of MALDI-MS (N_2 laser, 337 nm). This absorption provides useful applications of TCTS nanomagnets for LDI-MS such as surface enhanced laser desorption/ionization mass spectrometry (SELDI-MS).

The presence of thymine (T) in the chitosan nanomagnets is further confirmed using laser desorption/ionization mass spectrometry (LDI-MS) via direct spotting in the standard plate of conventional MALDI (Fig. 2d). Thymine has chemical formula ($C_5H_6N_2O_2$) with molecular weight of 126 g· mol^{-1}. LDI-MS shows peaks at 127, 149, 253, 275 and 291 Da corresponding to $[T + H]^+$, $[T + Na]^+$, $[2 T + H]^+$, $[2 T + Na]^+$, and $[2 T + K]^+$, respectively. The peak assignments are tabulated in Table S1. Detection of T-T complex
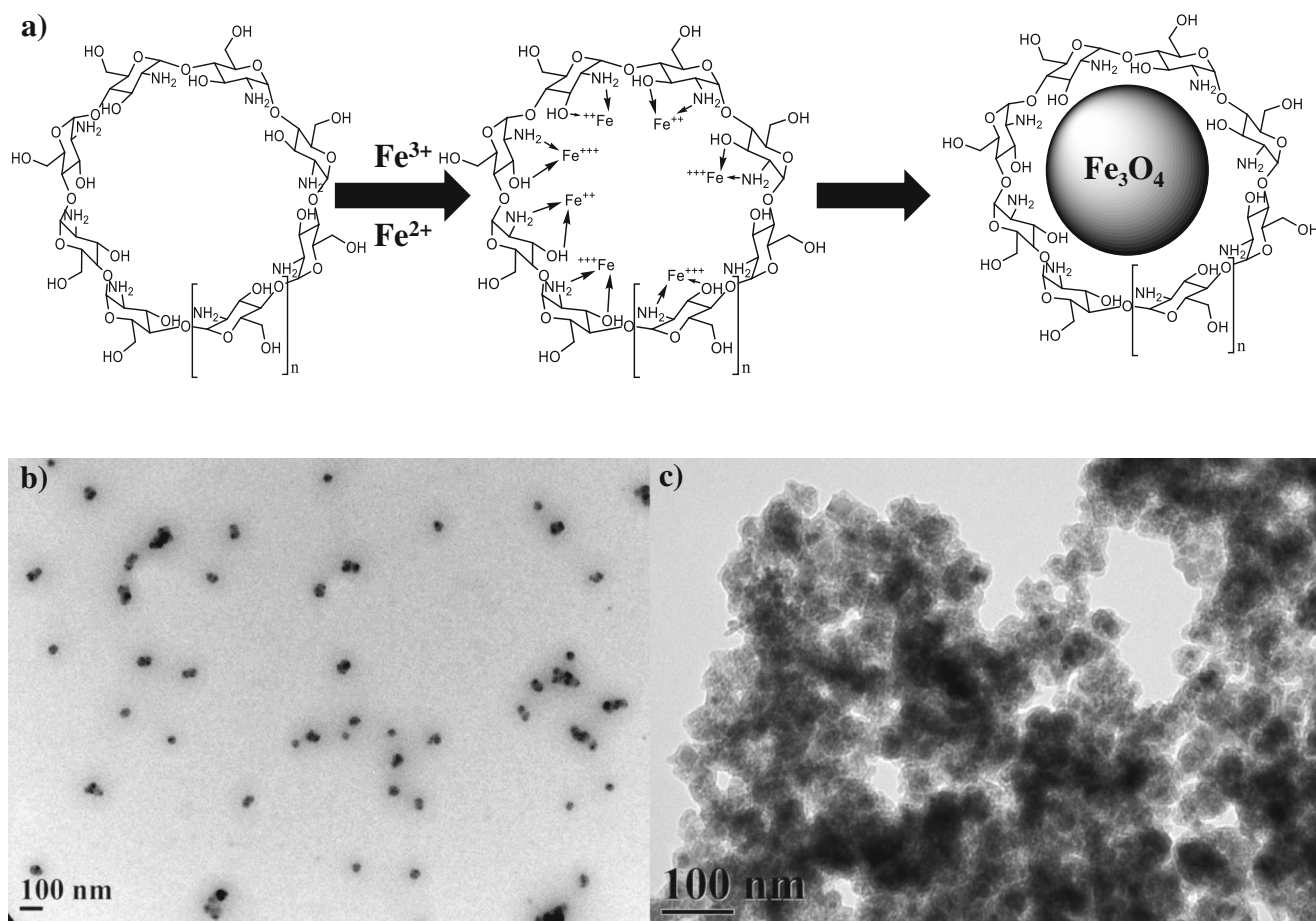
Fig. 1 **a** Schematic representation the synthesis of TCTS nanomagnets and TEM image for **b** CTS nanomagnets (CTS@Fe₃O₄) and **c**TCTS nanomagnets (TCTS@Fe₃O₄)

reveals the high softness of TCTS nanomagnets as surface for the applications of SELDI-MS. This property reveals the promising of the current method for mercury biosensing using thymine as chelating agent.

Selectivity and sensitivity

Natural Hg isotopes are a potent neurotoxin and were considered as the most highly toxic element. Mercury detection in the environment is reported as marker for pollution. The major challenge of mercury detection or sensing is that the element concentration is low and below the limit of detection (LOD) for many analytical techniques. A technique based on mass spectrometry such as MALDI-MS suffers from the matrix interferences in the low molecular weight region (50–500 m/z). Overall view of the separation of mercury ions (Hg(II)) using thymine modified chitosan nanomagnets (TCTS nanomagnets) and detection using LDI-MS is represented as shown in Fig. 3.

Chitosan is aminopolysaccharide of β-(1–4)-linked D-glucosamine (deacetylated unit) and N-acetyl-D-glucosamine (acetylated unit). It has many function groups

which served as chelating groups for transition metals. It serves as good stabilizing agent for magnetic nanoparticles and prevents aggregation via dipole-dipole interactions. Chitosan has been used for metal adsorption with high capacity. Thermodynamic analysis of Hg(II) chitosan interactions revealed that the adsorption is a spontaneous, fast and preferred process ($\Delta G° < 0$, $\Delta H° > 0$, $\Delta S° > 0$) [39]. However, chitosan lacks of selectivity. Thus, we modified chitosan nanomagnets with thymine (T) that has specific interaction with mercury (Hg(II)) as shown in Fig. 3. The non-covalent modification of chitosan with thymine is a request for LDI-MS. Mercury interaction with 10 bases pair double-stranded DNA duplex was investigated using extended X-ray absorption spectroscopy (EXAFS) [40]. EXAFS data showed that mercury Hg atom binding directly to a six-member ring, with a slight preference for the binding being to the N atom in thymine's pyrimidine ring. Moreover, EXAFS lacks of the clear distinguish between N or O atom in thymine ring. Nuclear magnetic resonance (NMR), electrospray ionization mass spectrometry (ESI-MS) and elemental analysis were used to study the interactions of Hg(II)-DNA duplexes [41]. Data revealed that thymine residues bind to Hg(II) through
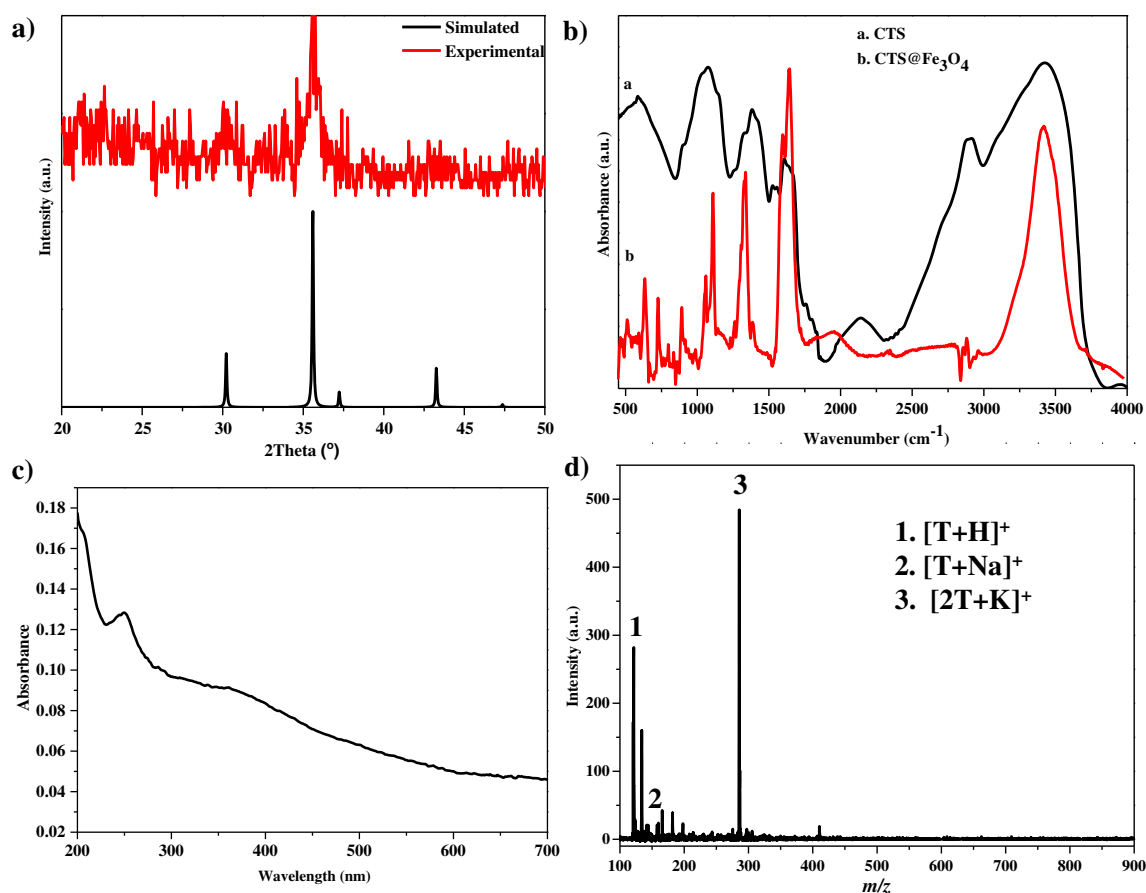
Fig. 2 Characterization of TCTS nanomagnets using **a** XRD, **b** FTIR, **c** UV-vis, and d) LDI-MS

covalent N—Hg bonds [41]. The elemental analysis of this complex showed that two HCl molecules disappear during the process for complex formation [41]. Hg(II) ions binds directly to N_3 of thymidine in place of the imino proton and bridges two thymidine residues to form the T-Hg-T pair [41].

A comparison between conventional organic matrix (2,5-DHB), thymine modified chitosan nanomagnets and combination of 2,5-DHB with thymine modified chitosan nanomagnets is shown in Fig. 4. MALDI-MS using conventional matrix (2,5-DHB) usually form undesirable interferences in low mass range (50–500 m/z). Furthermore, the matrix acidity destroys non-covalent and weak interactions in metal complexes. 2,5-DHB has chemical formula ($C_7H_6O_4$) with molecular weight 154 g·mol^{-1}. Self-ionization of 2,5-DHB in the presence of T-Hg-T complexes shows peaks at 177 and 137 m/z corresponding to [DHB + Na]$^+$ and [DHB-H_2O + H]$^+$ (Fig. 4). Data shows complexation of Hg(II) with T using DHB however of its acidity. This observation is due to the strong interaction of T-Hg-T complex. Furthermore, TCTS nanomagnets offers soft ionization and reveal complexation peak at 491 m/z corresponding to [Hg(T)$_2$(H$_2$O)$_2$ + H]$^+$ (Fig. 4). TCTS shows absence of T peak at 127 m/z that refers to [T + H]$^+$ compared to DHB or DHB and TCTS nanomagnets. This observation is due to the formation of

[Hg(T)$_2$(H$_2$O)$_2$ + H]$^+$. Chemical structures of DHB, T and its complexes with Hg(II) ions are represented in Fig. S1. TCTS nanomagnets could be used as matrix for LDI-MS because its UV-vis absorption matches with the laser wavelength of MALDI-MS instrument (337 nm). The large surface area of magnetic nanoparticles serves as surface for SALDI-MS. The combination between large surface area and UV absorption (337 nm) are preferable coined as SELDI-MS.

Using TCTS nanomagnets as preconcentration nanoprobe and matrix, detection of Hg(II) in standard solution are represented as shown in Fig. 5a. Data shows characteristic peaks at 491 and 455 m/z that are assigned to [Hg(T)$_2$(H$_2$O)$_2$ + H]$^+$ and [Hg(T)$_2$ + H]$^+$, respectively. In presence of other metals such as Fe (III), Fe (II), Cu (II), Mg (II), Ni (II), Hg(II), Na (I), K (I), Al (III), and Sn (IV), thymine binds specifically to Hg(II). This observation agree with other reports that showed high selectivity of Hg(II) to thymine base of DNA [41]. This method offers high sensitivity. Data shows that limit of detection (LOD) is 10 fmole which lower than the maximum contaminant level (MCL) of mercury(II) recommended for drinking water, i.e., 2 and 6 ppb, as established by U.S. Environmental Protection Agency (EPA, http://water.epa.gov/drink/contaminants/index.cfm#List) and the World Health Organization (WHO, 2011), respectively. Analysis of
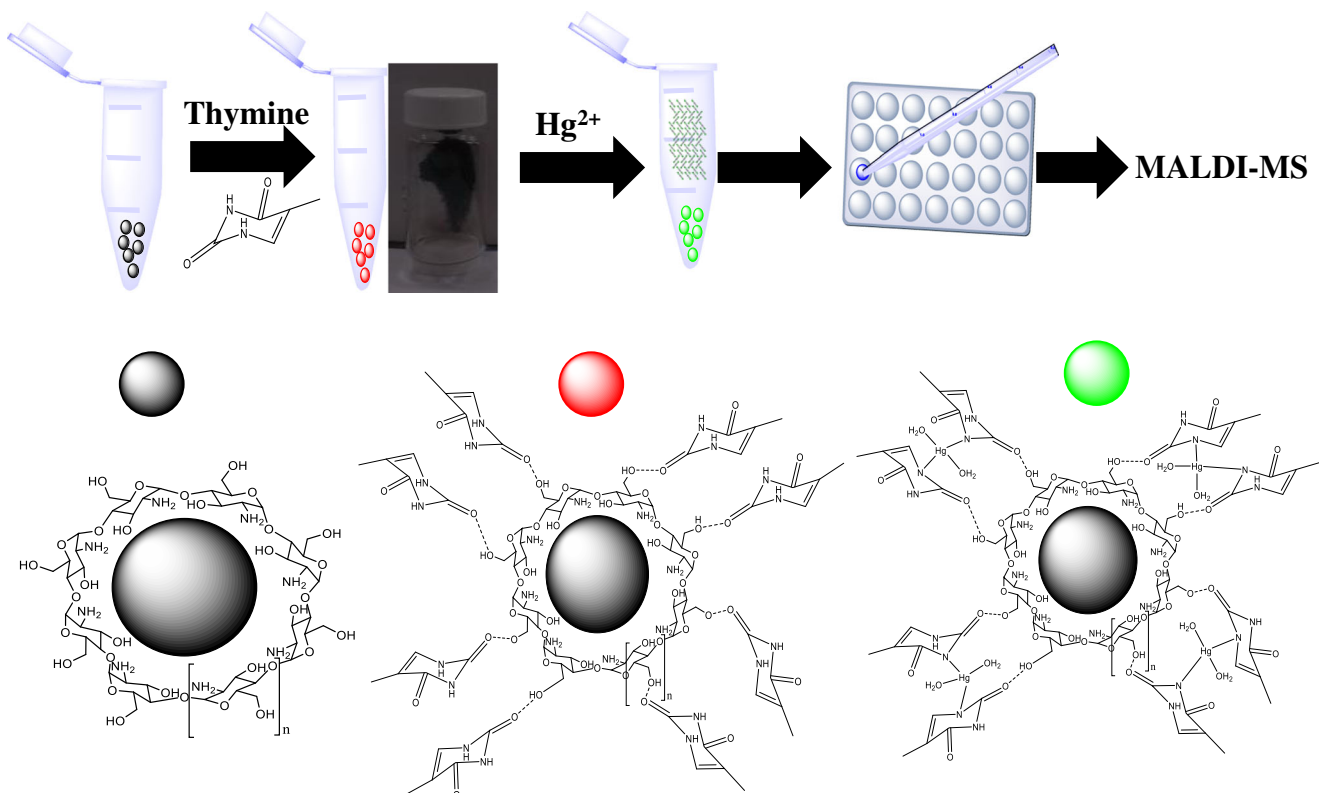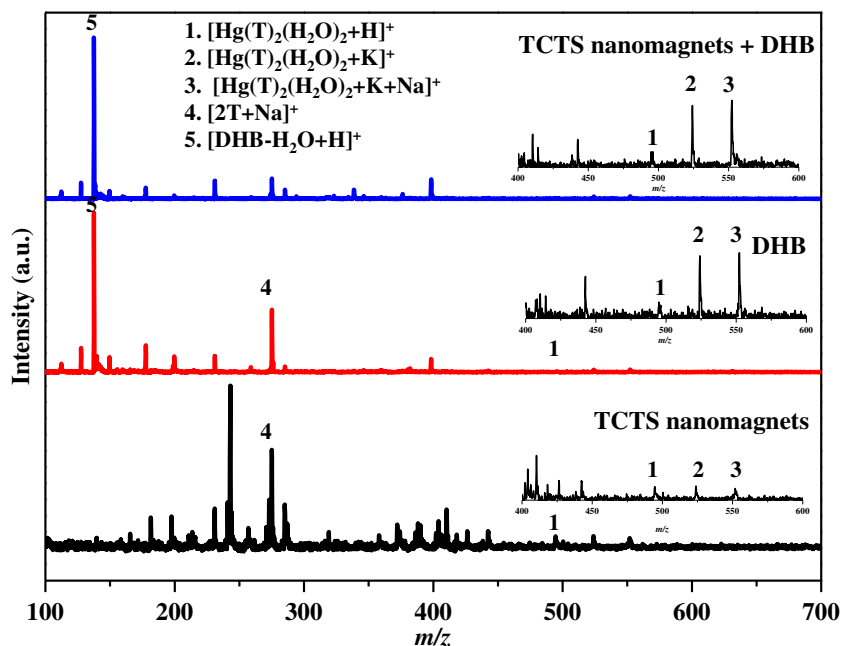
Fig. 3 Schematic representation of Hg^{2+} biosensing using TCTS nanomagnets followed by analysis using SELDI-MS

T-Hg-T using DHB in the presence of T and TCTS nanomagnets combination with DHB was reported as shown in Fig. S2 and Fig. S3, respectively. Data support the high performance of TCTS nanomagnets compared to the direct spotting of T with Hg(II) and using DHB as matrix.

Comparison between the current approach (thymine modified chitosan nanomagnets) and our previous technique (graphene assisted laser desorption/ionization mass spectrometry, GALDI-MS) is shown in Fig. 6. Mercury has seven stable isotopes with the following abundances according to the

Fig. 4 Analysis of Hg(II) as T-Hg-T using TCTS nanomagnets, conventional organic matrix (DHB) and co-matrix of TCTS nanomagnets and DHB

1. [Hg(T)$_2$(H$_2$O)$_2$+H]$^+$
2. [Hg(T)$_2$(H$_2$O)$_2$+K]$^+$
3. [Hg(T)$_2$(H$_2$O)$_2$+K+Na]$^+$
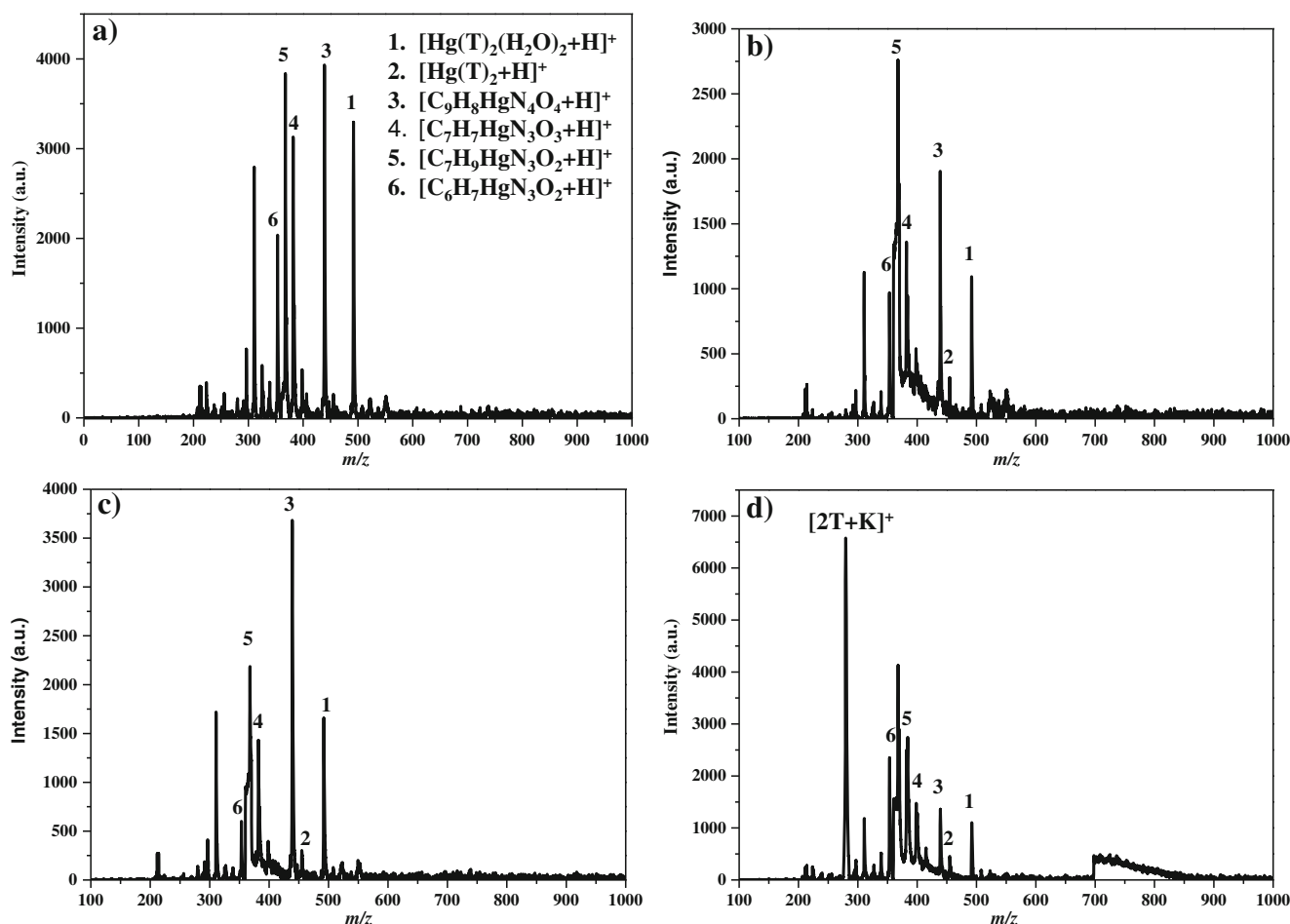4. [2T+Na]$^+$
5. [DHB-H$_2$O+H]$^+$

Fig. 5 Selectivity of TCTS nanomagnets for T-Hg-T analysis, **a** standard solution, **b** in the presence of Na (I), K (I), Fe (II), Cu (II), Mg (II), Ni (II), **c** in the presence of trivalent and **d** in the presence of all ions

National Institute of Standards and Technology (NIST) Standard References Material (SRM) 3133: ^{196}Hg, ^{198}Hg, ^{199}Hg, ^{200}Hg, ^{201}Hg, ^{202}Hg, and ^{204}Hg with percentage of 0.16%, 10.04%, 16.94%, 23.14%, 13.17%, 29.73%, and 6.83%, respectively [42]. Based on simulated mass spectrum (Fig. 6b), ionization of thymine complex with Hg(II) ions shows peaks at 484, 485, 486, 487, 488, 489 , 490, 491, 492, 493, 494 with intensity 0.1, 0.5, 0.1, 31.8, 57.5, 80.1, 51.8, 100, 12.8, 23.2, 2.9, 0.4, respectively. The chemical formula of this complex is $C_{10}H_{16}HgN_4O_6$ with molecular weight and mono-isotopic mass equal to 488.86 and 490.08 g·mol^{-1}, respectively that in good agreement with the simulated mass pattern (Fig. 6a). TCTS nanomagnets (Fig. 6b) and GALDI-MS (Fig. 6c) show good agreements with the simulated mass spectrum (Fig. 6a). TCTS nanomagnets assisted laser desorption/ ionization mass spectrometry technique shows lower resolution than GALDI-MS. However, the former is softer than the latter method. This claim is confirmed from the high intensity of T-Hg-T complex i.e. [Hg(T)$_2$(H$_2$O)$_2$ + H]$^+$ (Fig. 6). It is supported from the absence of peak at 470 m/z corresponding to [Hg(T)$_2$(H$_2$O) + H]$^+$ that is the parent peak in GALDI-MS

spectrum (Fig. 6c). TCTS nanomagnets offer separation facilities using simple magnetic field that is absent for GALDI-MS.

Analysis of real samples

Two different real samples; tap and sea water were used to approve the technique applicability. TCTS nanomagnets are useful as nanoprobe for preconcentration and as surface for SALDI-MS applications. Analysis of tap water (Fig. S4) and sea water (Fig. S5) using spike of standard mercury ions were investigated. Data shows successful detection of Hg as T-Hg-T (Fig. S4-S5). Limit of detection for tap water and sea water is 0.1 pmol and 1 pmol, respectively (Fig. S4-S5). Sea water has high salinity, so that it form clusters ions of K (I) and Na (I) as shown in Fig. S5 (peak at 553 m/z is assigned as [Hg(T)$_2$(H$_2$O)$_2$ + K + Na]$^+$).

Because of the dangerous character of Hg(II) ions for human being, monitoring technology should be fast, sensitive, and selective. The criterion of speed means that the results can be obtained in very short time. LDI-MS analysis using TCTS takes place in very short time (< 5 min). This technology
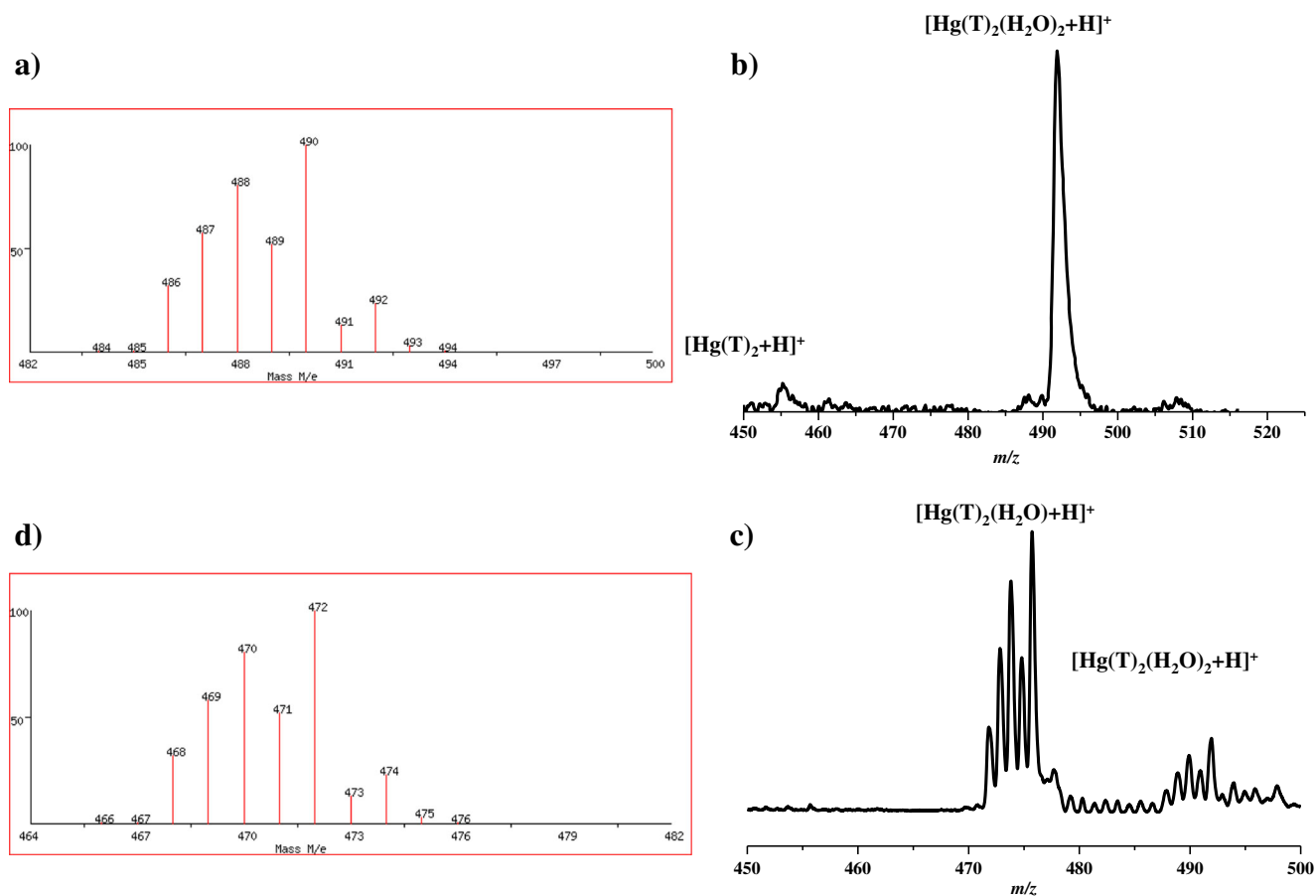
a)

b) $[Hg(T)_2(H_2O)_2+H]^+$

$[Hg(T)_2+H]^+$

d)

c) $[Hg(T)_2(H_2O)+H]^+$

$[Hg(T)_2(H_2O)_2+H]^+$

Fig. 6 Simulated peak mass pattern for peak $[Hg(T)_2(H_2O)_2 + H]^+$ at 491 *m/z* **a** and $[Hg(T)_2(H_2O) + H]^+$ at 472 *m/z*, comparison between **b** TCTS nanomagnets and **c** GALDI-MS

Table 1 Comparison among TCTS nanomagnets and other reported techniques

Material	Technique	LOD[a]	Linearity[a]	Time	Disadvantages	Mechanism	Ref
ODN–CDs	Fluorescence	2.6	5–200		Lack of high stability Required expensive ODN	The fluorescence of resultant ODN–CDs was quenched by GO via fluorescence resonance energy transfer. In the presence of Hg (II), the fluorescence was recovered	[14]
DNAzyme		2.4	2.4–20	> 8 min	Time dependent Expensive Require UO_2^{2+}	DNAzyme biocatalytic activity	[50]
Oligonucleotide functionalized magnetic silica sphere (MSS) @Au nanoparticles	SERS	10	0.1–1000	> 270 min	Interference from other ions	Detect complexes based on T-Hg-T	[17]
Laser breakdown time of flight mass spectrometry	Laser breakdown time of flight mass spectrometry	~30000			Require high energy and expensive	Atomic emission spectroscopy	[49]
Reduced graphene oxide	LDI-MS	2000		< 5 min	Require internal standard for quantification analysis	Detect T-Hg-T complex	[19]
TCTS nanomagnets		1		< 5 min			Here

a, nM; CDs-labeled oligodeoxyribonucleotide (ODN–CDs); oligonucleotide-functionalized magnetic silica sphere (MSS)@Au nano,: SERS. surface enhanced Raman spectroscopy; MALDI-MS, matrix assisted laser desorption/ionization mass spectrometry;

offers high throughput as over than 96 samples can be analysis in each single experiment. This technology (TCTS nanomagnets enhanced LDI-MS) requires very small volume (1–10 μL). TCTS nanomagnets enhanced LDI-MS shows high sensitivity and offers limit of detection levels of Hg(II) contamination below regulated dangerous human health levels. Finally, this technology shows highly selectivity in the sense of responding positively only to the targeted element e.g. Hg(II) ions. According to thermodynamic analysis (ΔG^0, ΔH^0, ΔS^0), the process of interactions of Hg(II) and CTS is spontaneous and preferable process [43]. These interactions are higher for TCTS compared to CTS. This method requires no DNA or any amplification [44]. It is important to mention that this method can be applied at various pH values because the addition of Hg stabilized duplex formation for the entire pH range tested [41].

MALDI-MS provides a simple analytical methods compared to many other techniques [45–48] . There are many methods and technique in literature for mercury detection or sensing. Comparison among the present method and other reported methods was tabulated in Table 1. Laser breakdown time of flight mass spectrometry was used for the detection of mercury and iodine [49]. This method is rapid and showed limit of detection equal to 0.82 ppb. However, this method is based on atomic emission spectroscopy and required high energy. Catalytic DNA sensors showed high selectivity using the appropriated DNA sequence that offered a very high affinity to Hg(II) ions [50]. However, it required expensive DNA and fluorophore. It requires perfect matches to form stable base pairs. These requirements are not important for our protocol. TCTS nanomagnets offers simple and easy separation method that make it promising for detection [51].

Conclusions

Thymine modified chitosan nanomagnets (TCTS nanomagnets) was successfully synthesized and applied for Hg(II) biosensing via the selective formation of T-Hg-T complex. TCTS nanomagnets served as nanoprobe for specific capture of Hg(II) ions, preconcentration probe and a surface for surface enhanced laser desorption/ionization mass spectrometry (SELDI-MS). This method is specific for Hg(II) compared to other ions. It is simple, required small volume, offers low limit of detection, and high throughput. The current approach is require no expensive reagents such as DNA, aptamers or others. The spectra of MS offers many peaks related to Hg(II) ions that provides precisely detection of these species. The current approach is applicable for real sample analysis.

References

1. Guallar E, Sanz-Gallardo MI, van't Veer P, Bode P, Aro A, Gómez-Aracena J, Kark JD, Riemersma RA, Martín-Moreno JM, Kok FJ (2002) Mercury, fish oils, and the risk of myocardial infarction. N Engl J Med 347:1747–1754. doi:10.1056/NEJMoa020157

2. Harris HH, Pickering IJ, George GN (2003) The chemical form of mercury in fish. Science 301:1203. doi:10.1126/science.1085941

3. Pacyna EG, Pacyna JM, Sundseth K, Munthe J, Kindbom K, Wilson S, Steenhuisen F, Maxson P (2010) Global emission of mercury to the atmosphere from anthropogenic sources in 2005 and projections to 2020. Atmos Environ 44:2487–2499. doi:10.1016/j.atmosenv.2009.06.009

4. Lamborg CH, Hammerschmidt CR, Bowman KL, Swarr GJ, Munson KM, Ohnemus DC, Lam PJ, Heimbürger LE, Rijkenberg MJA, Saito MA (2014) A global ocean inventory of anthropogenic mercury based on water column measurements. Nature 512:65–68. doi:10.1038/nature13563

5. UNEP (United Nations Environment Programme) (2013) Mercury_Time To Act http://www.unep.org/PDF/PressReleases/Mercury_TimeToAct.pdf. Accessed 6 Mar 2016

6. Legrand M, Passos CJS, Mergler D, Chan HM (2005) Biomonitoring of mercury exposure with single human hair strand. Environ Sci Technol 39:4594–4598. doi:10.1021/es047996o

7. Ammann AA (2007) Inductively coupled plasma mass spectrometry (ICP MS): a versatile tool. J Mass Spectrom 42:419–427. doi:10.1002/jms.1206

8. de Quadros DPC, Campanella B, Onor M, Bramanti E, Borges DLG, D'Ulivo A (2014) Mercury speciation by high-performance liquid chromatography atomic fluorescence spectrometry using an integrated microwave/UV interface. Optimization of a single step procedure for the simultaneous photo-oxidation of mercury species and photo-generation. Spectrochim Acta Part B At Spectrosc 101:312–319. doi:10.1016/j.sab.2014.09.019

9. Noor AM, Rameshkumar P, Huang NM, Wei LS (2016) Visual and spectrophotometric determination of mercury(II) using silver nanoparticles modified with graphene oxide. Microchim Acta 183:597–603. doi:10.1007/s00604-015-1680-8

10. Tang J, Huang Y, Zhang C, Liu H, Tang D (2016) DNA-based electrochemical determination of mercury(II) by exploiting the catalytic formation of gold amalgam and of silver nanoparticles. Microchim Acta 183:1805–1812. doi:10.1007/s00604-016-1813-8

11. Zhang J, Tang Y, Lv J, Fang S, Tang D (2015) Glucometer-based quantitative determination of Hg(II) using gold particle encapsulated invertase and strong thymine-Hg(II)-thymine interaction for signal amplification. Microchim Acta 182:1153–1159. doi:10.1007/s00604-014-1437-9

12. Kumari N, Dey N, Bhattacharya S (2014) Rhodamine based dual probes for selective detection of mercury and fluoride ions in water using two mutually independent sensing pathways. Analyst 139:2370–2378. doi:10.1039/c3an02020g

13. Abdelhamid HN, Wu H-F (2015) Reduced graphene oxide conjugate thymine as a new probe for ultrasensitive and selective fluorometric determination of mercury(II) ions. Microchim Acta 182:1609–1617. doi:10.1007/s00604-015-1461-4

14. Cui X, Zhu L, Wu J, Hou Y, Wang P, Wang Z, Yang M (2015) A fluorescent biosensor based on carbon dots-labeled oligodeoxyribonucleotide and graphene oxide for mercury (II) detection. Biosens Bioelectron 63:506–512. doi:10.1016/j.bios.2014.07.085

15. Wei Q, Nagi R, Sadeghi K, Feng S, Yan E, Ki SJ, Caire R, Tseng D, Ozcan A (2014) Detection and spatial mapping of mercury contamination in water samples using a smart-phone. ACS Nano 8:1121–1129. doi:10.1021/nn406571t

16. Liu X, Wu Z, Zhang Q, Zhao W, Zong C, Gai H (2016) Single gold nanoparticle-based colorimetric detection of Picomolar mercury ion with dark-field microscopy. Anal Chem 88:2119–2124. doi:10.1021/acs.analchem.5b03653

17. Liu M, Wang Z, Zong S, Chen H, Zhu D, Wu L, Hu G, Cui Y (2014) SERS detection and removal of mercury(II)/silver(I) using oligonucleotide-functionalized core/shell magnetic silica sphere@Au nanoparticles. ACS Appl Mater Interfaces 6:7371–7379. doi:10.1021/am5006282

18. Guerrini L, Rodriguez-Loureiro I, Correa-Duarte MA, Lee YH, Ling XY, García de Abajo FJ, Alvarez-Puebla RA (2014) Chemical speciation of heavy metals by surface-enhanced Raman scattering spectroscopy: identification and quantification of inorganic- and methyl-mercury in water. Nanoscale 6:8368–8375. doi:10.1039/c4nr01464b

19. Abdelhamid HN, Wu H-F (2014) Ultrasensitive, rapid, and selective detection of mercury using graphene assisted laser desorption/ionization mass spectrometry. J Am Soc Mass Spectrom 25:861–868. doi:10.1007/s13361-014-0825-z

20. Zhang Y, Xie J, Liu Y, Pang P, Feng L, Wang H, Wu Z, Yang W (2015) Simple and signal-off electrochemical biosensor for mercury(II) based on thymine-mercury-thymine hybridization directly on graphene. Electrochim Acta 170:210–217. doi:10.1016/j.electacta.2015.04.152

21. Lu M, Xiao R, Zhang X, Niu J, Zhang X, Wang Y (2016) Novel electrochemical sensing platform for quantitative monitoring of Hg(II) on DNA-assembled graphene oxide with target recycling. Biosens Bioelectron 85:267–271. doi:10.1016/j.bios.2016.05.027

22. Huber J, Leopold K (2016) Nanomaterial-based strategies for enhanced mercury trace analysis in environmental and drinking waters. TrAC Trends Anal Chem 80:280–292. doi:10.1016/j.trac.2015.09.007

23. Cui L, Guo X, Wei Q, Wang Y, Gao L, Yan L, Yan T, Du B (2015) Removal of mercury and methylene blue from aqueous solution by xanthate functionalized magnetic graphene oxide: sorption kinetic and uptake mechanism. J Colloid Interface Sci 439:112–120. doi:10.1016/j.jcis.2014.10.019

24. Jung JH, Lee JH, Shinkai S (2011) Functionalized magnetic nanoparticles as chemosensors and adsorbents for toxic metal ions in environmental and biological fields. Chem Soc Rev 40:4464–4474. doi:10.1039/c1cs15051k

25. Reddy DHK, Lee S-M (2013) Application of magnetic chitosan composites for the removal of toxic metal and dyes from aqueous solutions. Adv Colloid Interf Sci 201–202:68–93. doi:10.1016/j.cis.2013.10.002

26. Abdelhamid HN, Wu H-F (2013) Multifunctional graphene magnetic nanosheet decorated with chitosan for highly sensitive detection of pathogenic bacteria. J Mater Chem B 1:3950–3961. doi:10.1039/c3tb20413h

27. Hummers WS, Offeman RE (1958) Preparation of graphitic oxide. J Am Chem Soc 80:1339–1339. doi:10.1021/ja01539a017

28. Abdelhamid HN, Wu H-F (2012) A method to detect metal-drug complexes and their interactions with pathogenic bacteria via graphene nanosheet assist laser desorption/ionization mass spectrometry and biosensors. Anal Chim Acta 751:94–104. doi:10.1016/j.aca.2012.09.012

29. Abdelhamid HN, Khan MS, Wu H-F (2014) Graphene oxide as a nanocarrier for gramicidin (GOGD) for high antibacterial performance. RSC Adv 4:50035–50046. doi:10.1039/C4RA07250B

30. Abdelhamid HN, Wu B-S, Wu H-F (2014) Graphene coated silica applied for high ionization matrix assisted laser desorption/ionization mass spectrometry: a novel approach for environmental and biomolecule analysis. Talanta 126:27–37

31. Abdelhamid HN, Wu H-F (2015) Synthesis and characterization of quantum dots for application in laser soft desorption/ionization mass spectrometry to detect labile metal–drug interactions and their antibacterial activity. RSC Adv 5:76107–76115. doi:10.1039/C5RA11301F

32. Abdelhamid HN, Kumaran S, Wu H-F (2016) One-pot synthesis of CuFeO 2 nanoparticles capped with glycerol and proteomic analysis of their nanocytotoxicity against fungi. RSC Adv 6:97629–97635. doi:10.1039/C6RA13396G

33. Gopal J, Abdelhamid HN, Hua P-Y, Wu H-F (2013) Chitosan nanomagnets for effective extraction and sensitive mass spectrometric detection of pathogenic bacterial endotoxin from human urine. J Mater Chem B 1:2463–2475. doi:10.1039/c3tb20079e

34. Chen Z-Y, Abdelhamid HN, Wu H-F (2016) Effect of surface capping of quantum dots (CdTe) on proteomics. Rapid Commun Mass Spectrom 30:1403–1412. doi:10.1002/rcm.7575

35. Nasser Abdelhamid H, Wu HF (2013) Furoic and mefenamic acids as new matrices for matrix assisted laser desorption/ionization-(MALDI)-mass spectrometry. Talanta 115:442–450. doi:10.1016/j.talanta.2013.05.050

36. Abdelhamid HN, Bhaisare ML, Wu H-F (2014) Ceria nanocubic-ultrasonication assisted dispersive liquid-liquid microextraction coupled with matrix assisted laser desorption/ionization mass spectrometry for pathogenic bacteria analysis. Talanta 120:208–217. doi:10.1016/j.talanta.2013.11.078

37. Li G, Jiang Y, Huang K et al (2008) Preparation and properties of magnetic Fe3O4–chitosan nanoparticles. J Alloys Compd 466:451–456. doi:10.1016/j.jallcom.2007.11.100

38. Kuo C-H, Liu Y-C, Chang C-MJ, Chen JH, Chang C, Shieh CJ (2012) Optimum conditions for lipase immobilization on chitosan-coated Fe3O4 nanoparticles. Carbohydr Polym 87:2538–2545. doi:10.1016/j.carbpol.2011.11.026

39. Kyzas GZ, Deliyanni EA (2013) Mercury(II) removal with modified magnetic chitosan adsorbents. Molecules 18:6193–6214. doi:10.3390/molecules18066193

40. Ravel B, Slimmer SC, Meng X, Wong GCL, Lu Y (2009) EXAFS studies of catalytic DNA sensors for mercury contamination of water. Radiat Phys Chem 78:S75–S79. doi:10.1016/j.radphyschem.2009.05.024

41. Miyake Y, Togashi H, Tashiro M, Yamaguchi H, Oda S, Kudo M, Tanaka Y, Kondo Y, Sawa R, Fujimoto T, Machinami T, Ono A (2006) MercuryII-mediated formation of thymine-HgII-thymine base pairs in DNA duplexes. J Am Chem Soc 128:2172–2173. doi:10.1021/ja056354d

42. Blum JD, Sherman LS, Johnson MW (2014) Mercury isotopes in earth and environmental sciences. Annu Rev Earth Planet Sci 42:249–269. doi:10.1146/annurev-earth-050212-124107

43. Kyzas GZ, Travlou NA, Deliyanni EA (2014) The role of chitosan as nanofiller of graphite oxide for the removal of toxic mercury ions. Colloids Surf B: Biointerfaces 113:467–476. doi:10.1016/j.colsurfb.2013.07.055

44. Zhu M, Wang Y, Deng Y, Yao L, Adeloju SB, Pan D, Xue F, Wu Y, Zheng L, Chen W (2014) Ultrasensitive detection of mercury with a novel one-step signal amplified lateral flow strip based on gold nanoparticle-labeled ssDNA recognition and enhancement probes. Biosens Bioelectron 61:14–20. doi:10.1016/j.bios.2014.04.049

45. Abdelhamid HN, Wu H-F (2014) Facile synthesis of nano silver ferrite (AgFeO2) modified with chitosan applied for biothiol

separation. Mater Sci Eng C Mater Biol Appl 45:438–445. doi:10.1016/j.msec.2014.08.071

46. Abdelhamid HN, Talib A, Wu H-F (2015) Facile synthesis of water soluble silver ferrite (AgFeO2) nanoparticles and their biological application as antibacterial agents. RSC Adv 5:34594–34602

47. Abdelhamid HN, Wu H-F (2014) Proteomics analysis of the mode of antibacterial action of nanoparticles and their interactions with proteins. TrAC Trends Anal Chem 65:30–46

48. Abdelhamid HN, Wu H-F (2013) Probing the interactions of chitosan capped CdS quantum dots with pathogenic bacteria and their biosensing application. J Mater Chem B 1:6094–6106. doi:10.1039/c3tb21020k

49. Wang ZZ, Deguchi Y, Yan JJ, Liu JP (2014) Rapid detection of mercury and iodine using laser breakdown time-of-flight mass spectrometry. Spectrosc Lett 48:128–138. doi:10.1080/00387010.2013.859158

50. Liu J, Lu Y (2007) Rational design of "turn-on" allosteric DNAzyme catalytic beacons for aqueous mercury ions with ultra-high sensitivity and selectivity. Angew Chem 119:7731–7734. doi:10.1002/ange.200702006

51. Wang H, Chen B, Zhu S, Yu X, He M, Hu B (2016) Chip-based magnetic solid-phase microextraction online coupled with MicroHPLC-ICPMS for the determination of mercury species in cells. Anal Chem 88:796–802. doi:10.1021/acs.analchem.5b03130